International Journal of Engineering Research & Technology (IJERT)
ISSN: 2278-0181
Vol. 9 Issue 05, May-2020

$Fe_{0.986}Ru_{0.014}S_2$ Thin Films, Having Desired Properties for Photovoltaic Application, Synthesized by Spray Pyrolysis Technique

Beya Ouertani[a,b,*], Belguecem Tiss[c], Mohamed Ben Rabeh[d], Wissem Cheikhrouhou-Koubaa[e], Hatem Ezzaouia[a]

[a] Semi conductor and Advanced Technology Nanostructured Laboratory, Research and Technology Center on Energy, Borj-Cedria Science and Technology Park, BP, 95, 2050 Hammam-Lif, Tunisia.

[b] University of Carthage, Higher Institute of Environmental Sciences and Technologies of Borj Cedria, Borj-Cedria Science and Technology Park, Tunisia.

[c] University of Gabes, Faculty of Sciences in Gabes, Laboratory of Physics of Materials and Nanomaterials Applied at Environment, 6072, Gabes, Tunisia.

[d] Université de Tunis El Manar, Ecole Nationale d'Ingénieurs de Tunis, Laboratoire de Photovoltaïques et Matériaux Semi-conducteurs, BP 37 Le Bélvédère 1002, Tunis, Tunisia.

[e] Laboratory of Technologies for Smarts Systems, Numeric Research Center, Sfax Technopark, BP 275, 3021, Sakiet-ezzit, Tunisia

***Abstract*: - A good choice of the ruthenium doping percentage has given high-quality $Fe_{0.986}Ru_{0.014}S_2$ thin films having desired properties for several applications, such as photovoltaic. These layers have been grown by a simple and non toxic technique: spray pyrolysis. In a first step, for an adequate molar ratio of ($FeCl_3.6H_2O$: $RuCl_3.3H_2O$), amorphous Ru-doped iron oxide thin films were deposited on glass substrate pre-heated at 350°C. Then, a heat treatment at 450°C under sulfur atmosphere (~10^{-4} torr) in sealed-tube transformed the as obtained films into $Fe_{0.986}Ru_{0.014}S_2$ films. XRD analysis confirmed the FeS_2 phase. The estimated compositions were tested by the EDX analysis. Surface morphology is studied by SEM and AFM and the obtained images showed an inhomogeneous granular structure and a rough surface. However, the granular size varies from 150 nm to 300 nm. The optical measurements showed a high absorption coefficient ($\alpha > 3.5x10^4$ cm^{-1} for wave lengths lower than 800 nm). A direct band gad corresponding to a photon energy of 1.55 eV was obtained after plotting $(\alpha h\nu)^2$ versus the photon energy ($h\nu$); which is an estimated value for photovoltaic application. The electron mobility in $Fe_{0.986}Ru_{0.014}S_2$ films has been obtained from Hall Effect measurement where an initial current of 1µA and a magnetic field, B = 0.554T, are applied. Our layers show n-type conduction. Electrical measurements (bulk concentration $=1.0209x10^{+19}$ cm^{-3}, Sheet Concentration=2.766510^{+15} cm^{-2}) encourage their use as good low cost materials for solar cells. Indeed, the carrier mobility was measured of about 0.21215 $cm^2/(V.s)$, the resistivity was of 2.8821 Ω.cm, and the conductivity was of 0.34696 $Ω^{-1}.cm^{-1}$. The bulk concentration was of $1.0209×10^{19}cm^{-3}$.**

Keywords: Growth, characterization, Electrical, optical, low cost materials, spray pyrolysis, desired band gap.

1. INTRODUCTION:

Nowadays, researchers are of great interest to innovate new low cost materials for solar cells **[1-14]**. Several research works focused on the Pyrite films fabrication because of their low cost, but unconvincing results were obtained. However, for their use in this area, it needs to improve their properties (optical and electrical). Thus, researchers thought about their doping in the aim to improve their optical and electrical properties to make it more effective as a photovoltaic material. Different dopants were chosen As, Ni, Co, Cu, Al, Ni, Zn, Os, Ru, Mg, Ba, etc **[6, 15-24]**.

Knowing that, the ruthenium has been treated as a good candidate for doping FeS_2 thin films in the aim to improve their properties since they were chosen among the low cost materials for solar cells. Indeed, in a previous work **[19]**, a good study was done concerning the Ru-alloyed FeS_2 thin films for solar cells application wherein estimated optical results were obtained for the ratio $RuCl_3.3H_2O$**:**$FeCl_3.6H_2O$ of about 1.56% (high absorbance and a direct band gap corresponding to photon energy of 1.48 eV). In order to fabricate Ru-doped FeS_2 films having good properties for solar cells application, which means a good choice of the ratio: $RuCl_3.3H_2O$**:**$FeCl_3.6H_2O$; we tried with different ratios close to 1.56% **[19]**. Hence, a well chosen ratio: $RuCl_3.3H_2O$**:**$FeCl_3.6H_2O$ of 1.46% allowed us to fabricate $Fe_{0.986}Ru_{0.014}S_2$ thin films having desired optical and electrical properties for solar cells application.

2. GROWTH OF THE $FE_{0.98845}RU_{0.01155}S_2$ THIN FILMS:

Using the simple technique: spray pyrolysis, and non toxic and non cost precursors, amorphous Ru-doped iron oxide films were obtained by spraying $FeCl_3·6H_2O$ (0.03 M)-based aqueous solution onto pre-heated glass substrates (at 350°C) during 10 min; on which was sprayed, immediately, another layer of an aqueous solution of $RuCl_3·3H_2O$ (density=3.11 g/mL at 25 °C), during 1 min with the chosen molar ratio: $RuCl_3·3H_2O$:$FeCl_3·6H_2O$=x:1−x (x ≅ 0.0146).

International Journal of Engineering Research & Technology (IJERT)
ISSN: 2278-0181
Vol. 9 Issue 05, May-2020

The as obtained amorphous Ru-doped iron oxide films were transformed into $Fe_{(1-x)}Ru_xS_2$ films after heat treatment under sulfur atmosphere (~10^{-4} torr) at $T_{sulfuration}$ = 450°C for 3h. Dark films with good adherence to the substrate were obtained. Therefore, the prepared films are treated by XRD to identify the obtained phase, and then their optical properties are obtained after reflectivity and transmittance measurements. Electrical properties are obtained by Hall Effect technique. The surface morphology is investigated by SEM and AFM.

3. EXPERIMENTAL DETAILS:

3.1 Structural properties

a-X-ray diffraction

The adequate molar ratio (33 : 65 : 2) of ($FeCl_3.6H_2O$: S : $RuCl_3.3H_2O$) was used to synthesize Ru-doped FeS_2 material. The obtained phase was investigated by powder X-ray diffraction (PXRD) with a Bruker D8 Advance diffractometer equipped with a lynxeye detector. The dichromatic copper radiation ($CuK_{\alpha1/\alpha2}$) was used by the θ–2θ scan in the 2θ range of 5-70°. Full diffraction power of 40mA/40kV with 0.018° Δθ step and 2s time-step were used to record the diffraction pattern represented in Fig.1. The search-match phase identification procedure was applied using the Powder Diffraction File (PDF) database and the PanAlytical XpertPro Highscore software. Two phases were identified in the diffraction pattern: FeS_2 (JCPDS card n°: 00-024-0076) and Fe_2O_3. The sulfuration of the pre-deposited Ru-doped iron oxide layers under vacuum (~10^{-4} torr) takes 3h at 450°C.

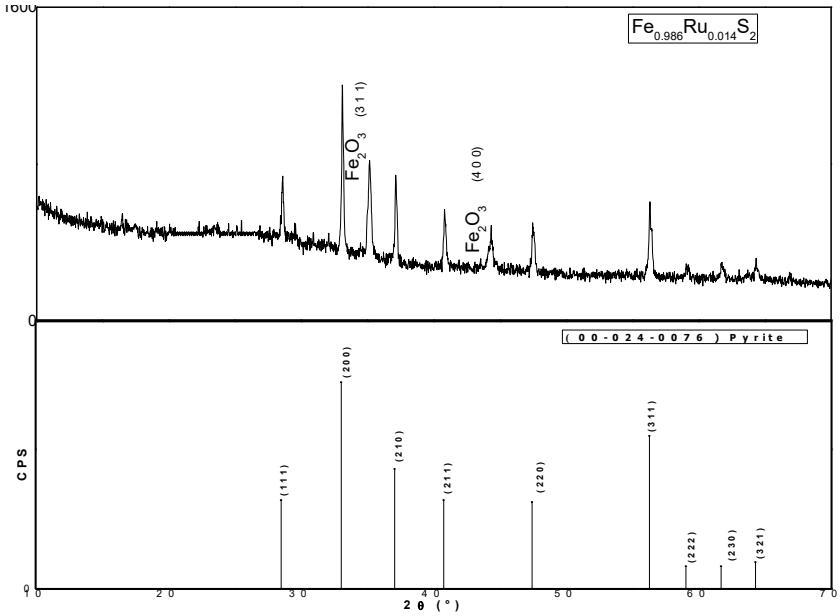

Fig.1 : XRD spectrum of the Ru-doped FeS_2 films obtained after heat treatment under sulfur atmosphere (~10^{-4} torr) at $T_{sulfuration}$ = 450°C for 3h of the amorphous Ru-doped iron oxide films that had been obtained according to the molar ratio: $RuCl_3{\cdot}3H_2O$:$FeCl_3{\cdot}6H_2O$=x:1−x (x ≅ 0.0146).

Compared to the initial pyrite peak position, the observed shift towards the low 2θ values of the obtained thin film proofs the ruthenium doping of the pyrite material and the synthesis of Ru-doped FeS_2. Since the ruthenium atomic radius is larger than that of the iron, replacing Fe by Ru will increase the cubic cell parameter explaining the observed shift of the Bragg peaks position. The refined cubic cell parameter of the Ru-doped FeS_2 is a = 5.4180 Å.

b-Energy Dispersive X-ray Spectroscopy (EDX or EDS) analysis:

To determine the compositions of the Ru-doped FeS_2 stacked layers, EDS analysis were carried out using a Thermo Scientific UltraDry Detector. The measured values are summarized in Table.1.

Table.1: EDS analysis of the Ru-doped FeS_2 films obtained after heat treatment under sulfur atmosphere (~10^{-4} torr) at $T_{sulfuration}$ = 450°C for 3h of the amorphous Ru-doped iron oxide films pre-deposited by spray pyrolysis according to the molar ratio: $RuCl_3{\cdot}3H_2O$:$FeCl_3{\cdot}6H_2O$=x:1−x (x ≅ 0.0146).

Element	*Net Counts*	*Weight %*	*Atom %*	*(Fe/S %)*	*(Ru/S %)*
S	42682	33.27	26.25	~0.4396 < 0.5	~0.0293
Fe	6104	25.49	11.54		
Ru	1655	3.08	0.77		

International Journal of Engineering Research & Technology (IJERT)
ISSN: 2278-0181
Vol. 9 Issue 05, May-2020

Since the ratio $\frac{Fe}{S} = 0.5$, the pyrite phase is stoichiometric represented by FeS_2. In this work, the observed ratio is slightly less than 0.5 ($\frac{Fe}{S} = 0.44$) in the obtained thin films. Using this ratio, the x value in the proposed formula ($Fe_{(1-x)}Ru_xS_2$) can be calculated from :

$$\frac{Ru}{S} = 2x \quad \Leftrightarrow \quad \frac{0.77}{26.25} = 2x \Rightarrow \quad x = 0.01465$$

However the new obtained Ru-doped FeS_2 phase formula is **$Fe_{0.986}Ru_{0.014}S_2$**.

3.2 Surface morphology

Scanning-electron-microscopy

The surface morphology of the $Fe_{0.986}Ru_{0.014}S_2$ films is visualized by a Thermo Scientific Q250 SEM. Fig.2 shows SEM micrographs surface views at different magnifications of Ru-alloyed pyrite films annealed at 450 °C under vacuum (~10^{-4} torr) for 3h.

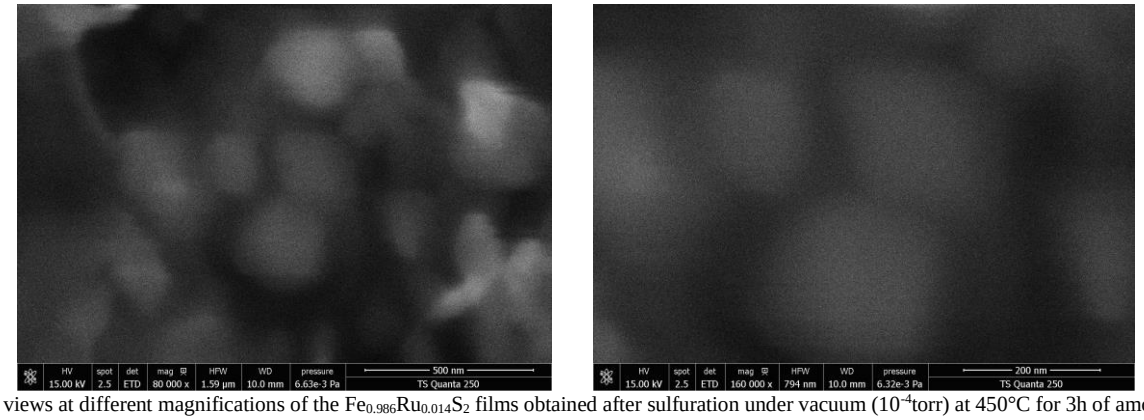

Fig.2: SEM views at different magnifications of the $Fe_{0.986}Ru_{0.014}S_2$ films obtained after sulfuration under vacuum (10^{-4}torr) at 450°C for 3h of amorphous Ru-doped FeS_2 films deposited on pre-heated glass substrates (at 350°C) for 10 min according to the adequate molar ratio (33 : 65 : 2) of ($FeCl_3.6H_2O$: S : $RuCl_3.3H_2O$).

Porous surface and inhomogeneous granular structure were shown. The grain size could reach 300 nm. These properties encourage more their application as solar cells.

Atomic-Force-Microscopy

To further investigate the morphology of the obtained films ($Fe_{0.986}Ru_{0.014}S_2$) a characterization by AFM (Dimension 3100 controller NanoscopeIIIa, Digital Instruments, Veeco, Metrology Group) in contact mode at ambient temperature was done. Root mean square (rms) surface roughness value was determined on an area of 2µm x 2µm for the studied films. The rms was calculated using the roughness analyses software provided by the instrument manufacturer. Fig. 3 shows AFM surface morphology of the $Fe_{0.986}Ru_{0.014}S_2$ film. A granular structure was observed confirming the SEM observation (Fig. 2).

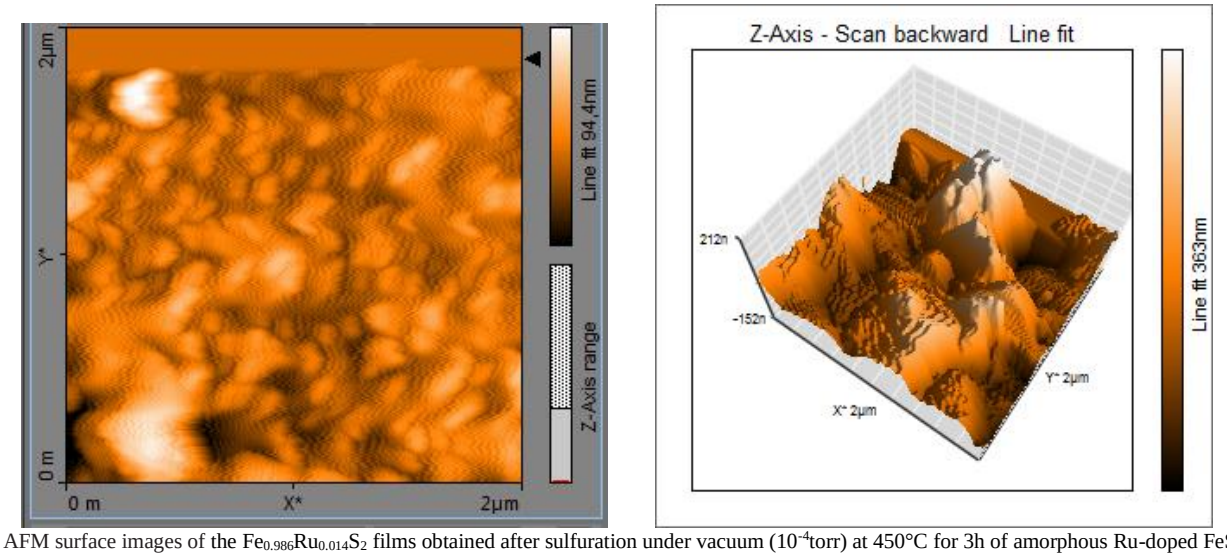

Fig.3 : AFM surface images of the $Fe_{0.986}Ru_{0.014}S_2$ films obtained after sulfuration under vacuum (10^{-4}torr) at 450°C for 3h of amorphous Ru-doped FeS_2 films deposited on pre-heated glass substrates (at 350°C) for 10 min according to the adequate molar ratio (33 : 65 : 2) of ($FeCl_3.6H_2O$: S : $RuCl_3.3H_2O$).

International Journal of Engineering Research & Technology (IJERT)
ISSN: 2278-0181
Vol. 9 Issue 05, May-2020

The AFM images of the obtained films show porous and rough surface (Fig. 3), a strong roughness was observed. AFM images (Fig. 3) are in agreement with SEM views, when irregular spherical crystallites and a large grain size dimensions were observed.

3.3 Optical Properties

Optical absorption spectra of the as-prepared non-doped and Ru-doped pyrite thin films were recorded using a SHIMADZU 3100S spectrophotometer. Fig.4 depicts the optical absorption spectra versus photon energy (hν). The transmission and reflectivity variations versus the wavelength (400 nm–1800nm) of the obtained films are shown in Fig.4 (a,b).

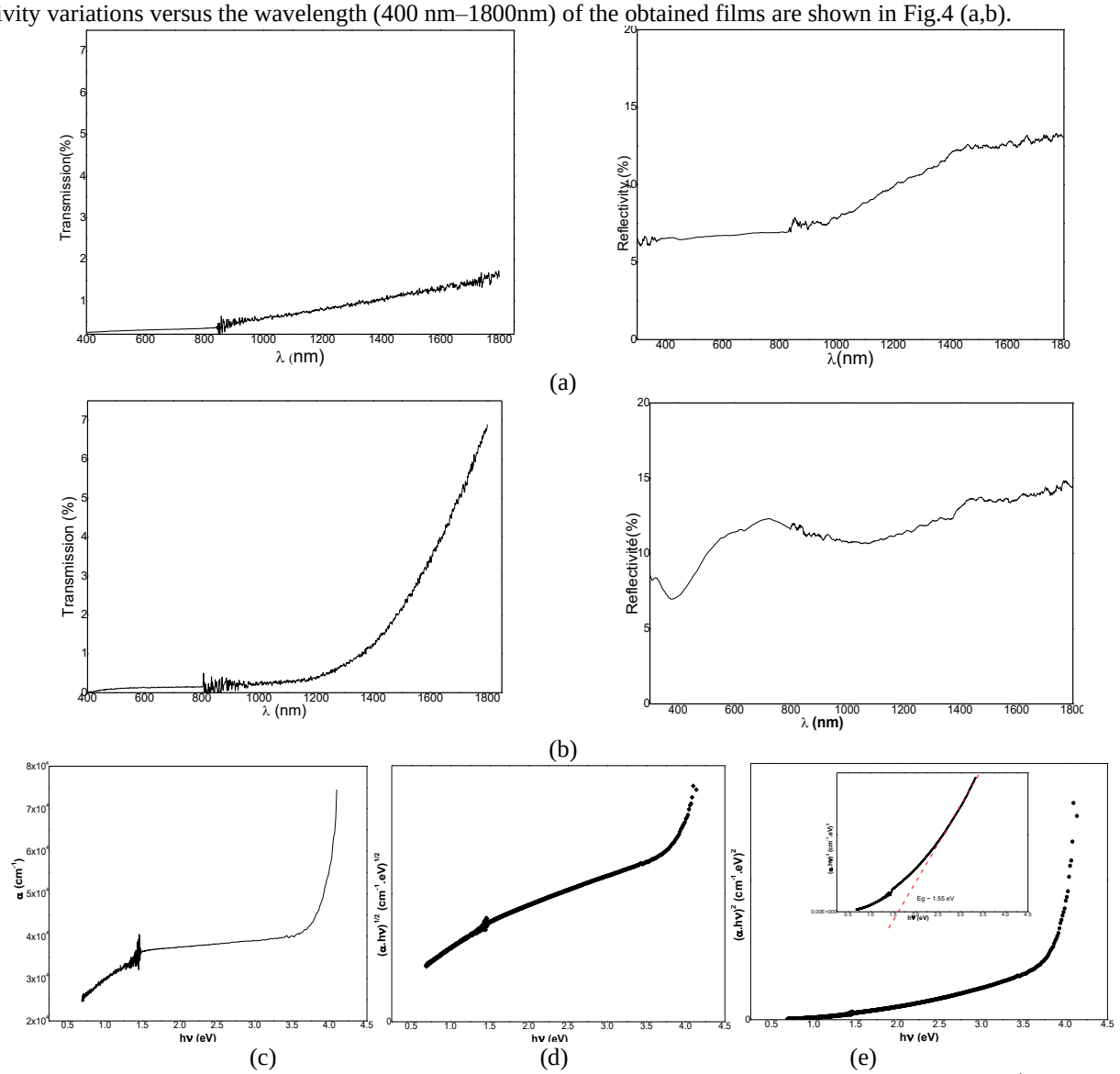

Fig.4: Optical absorption spectra of the $Fe_{0.986}Ru_{0.014}S_2$ (a,c,d, and e), and FeS_2 thin films (b), obtained after sulfuration under vacuum (10^{-4} torr) at 450°C for 3h of simultaneously amorphous Ru-doped iron oxide, and iron oxide films pre-deposited on heated glass substrates (at 350°C) by spray pyrolysis technique.

It appears that the transmission and reflectivity coefficients measurements of the $Fe_{0.986}Ru_{0.014}S_2$ films (Fig.4(a)) have shown a remarkable decrease comparing to those of the non doped FeS_2 films (Fig.4 (b)). However, the obtained $Fe_{0.986}Ru_{0.014}S_2$ films showed a high absorption coefficient ($\alpha > 2x10^4 cm^{-1}$ for $\lambda < 1900nm$) (Fig.4(c)). Plots of $(\alpha h\nu)^{n/2}$ versus the photon energy hν, with n=1 and n=4 for these obtained layers are given simultaneously in Fig.4(d) and Fig.4 (e). Three transitions are depicted: an indirect one corresponding to photon energy of about 2.8 eV and two direct ones corresponding to the energies 1.55 eV and 3.72 eV. Thus, the lower energy is attributed to a direct band gap of the $Fe_{0.986}Ru_{0.014}S_2$ phase comparing to the values range of the $Fe_{(1-x)}Ru_xS_2$ band gaps obtained previously [13]. The two other transitions, direct and indirect, corresponding to the energies 2.8 eV and 3.72 eV could be attributed to the iron oxide phases.

International Journal of Engineering Research & Technology (IJERT)
ISSN: 2278-0181
Vol. 9 Issue 05, May-2020

3.4 Electrical transport properties

To assess the electrical quality of the Ru-doped FeS_2 thin films, especially of the $Fe_{0.986}Ru_{0.014}S_2$ ones, Hall mobility measurements were performed and analyzed to extract carrier mobility and carrier concentration. The obtained carrier density (n) and mobility (μ_n) of an n-type semiconductor can be determined from the measured Hall coefficient ($R_H(B)$) and the resistivity ($\rho(B)$) using the relations:

$$n = \frac{r_H}{q.R_H(B)} \qquad (1)$$

and $$\mu_n = \frac{1}{n.q.\rho(B)} \qquad (2)$$

Where q is the electronic charge, B is the applied magnetic field, and r_H is the Hall factor.
In fact, the Hall coefficient R_H is given by the following equation:

$$R_H = \frac{V_H.t}{IB} = \frac{1}{ne} \qquad (3)$$

Recall that when electrons are the charge carriers, R_H is negative and when holes are the charge carriers, R_H is positive.
In the present work the electron mobility in the as obtained $Fe_{0.98535}Ru_{0.01465}S_2$ films has been obtained from Hall Effect measurement where an initial current of 1µA and a magnetic field, B = 0.554T are applied. Our layers show n-type conduction. The electrical measurements such as: the bulk concentration that is about $1.0209x10^{+19}$ cm^{-3}, and the sheet concentration that is of about 2.766510^{+15} cm^{-2}, encourage their use as good low cost materials for solar cells. Indeed, the carrier mobility was measured of about 0.21215 $cm^2/(V.s)$, the resistivity was of 2.8821 Ω.cm, and the conductivity was of 0.34696 $\Omega^{-1}.cm^{-1}$.

4. CONCLUSION:

An adequate molar ratio was chosen to fabricate $Fe_{0.986}Ru_{0.014}S_2$ thin films having good properties for solar cells application. The morphology study showed a granular structure with grain sizes reaching 300 nm, which means that our layers present a good porosity. A strong roughness was observed. The optical properties of these layers showed a high absorption coefficient ($\alpha > 2x10^4 cm^{-1}$ for λ < 1900nm) and a direct band gap corresponding to photon energy of 1.55 eV; which is considered as a desired band gap value for solar cells application. In addition, the obtained electrical properties of the $Fe_{0.986}Ru_{0.014}S_2$ layers were optimal for the intended application. Thus, one can say that the obtained $Fe_{0.986}Ru_{0.014}S_2$ thin layers could be used as a material for low cost solar cells application. It could be considered as an interesting plus in the field of low cost materials for solar cells application.

ACKNEWLEGMENTS :

We would like to thank deeply Pr. Habib Boughzala, « Laboratoire de Matériaux et Cristallochimie, Faculté des Sciences de Tunis (F.S.T), Université de Tunis El Manar » for his scientific helps and his support. Our deep thanks go to all the staff of the « Laboratoire de Photovoltaïque, Centre de Recherches et des Technologies de l'Énergie, Technopole de Borj-Cédria » and specially the Director, Pr. Mongi Bouaicha, for their support. Our deep gratitude and regard to Mr. Taoufik Bouaanane, technician in this same laboratory for his precious electrical measurements. We would like to take this opportunity to express our deep gratitude and regard to Pr. Kamel Khirouni and Pr. Noureddine Bouguila, Laboratory of Physics of Materials and Nanomaterials Applied at Environment-Faculty of Sciences in Gabes, for their support.

REFERENCES:

[1] Feng Zhao, YanLiang, Jeong BaeLee, and Seung J.Hwang, Materials Science and Engineering: B, Volume 248, (September 2019), 114404.
[2] Cheng Wang, Junsen Zhang, Liangxing Jiang, Li Gong, Haipeng Xie, Yongli Gao, Haiping He, Zhishan Fang, Jincheng Fan, Zisheng Chao, Journal of Alloys and Compounds, Volume 817, (15 March 2020), 152768.
[3] Khagendra P. Bhandari, Xinxuan Tan, Peymon Zereshki, Fadhil K. Alfadhili, Adam B. Phillips, Prakash Koirala, Michael J. Heben, Robert W. Collins, and Randy J. Ellingson, Solar Energy Materials and Solar Cells, Volume 163, (April 2017), Pages 277-284.
[4] Beau J. Richardson, Leize Zhu, and Qiuming Yu, Solar Energy Materials and Solar Cells, Volume 116, (September 2013), Pages 252-261.
[5] Ravi P. Srivastava, and Sarang Ingole, Materials Science in Semiconductor Processing, Volume 106, (February 2020), Article 104775.
[6] Tian-Lun Liu, and Jian-Min Zhang, Materials Chemistry and Physics, Volume 2441, (April 2020),Article 122742.
[7] B. Ouertani, J. Ouerfelli, M. Saadoun, M. Zribi, M.Ben Rabha, B. Bessaïs, H. Ezzaouia, Thin Solid Films 511 – 512 (2006) 457 – 462.
[8] B. Ouertani, J. Ouerfelli, M. Saadoun, B. Bessaïs, H. Ezzaouia, J.C. Bernède, Materials Characterization 54 (2005) 431– 437.
[9] A. Ennaoui, S. Fiechter, C. Pettenkofer, N. Alonsovance, K. Buker, M. Bronold, et al., Sol. Energy Mater. Sol. Cells 29 (4) (1993) 289–370.
[10] B. Ouertani, J. Ouerfelli, M. Saadoun, B. Bessaïs, H. Ezzaouia, J.C. Bernède, Solar Energy Materials & Solar Cells 87 (2005) 501–511.
[11] B. Ouertani, J. Ouerfelli, M. Saadoun, B. Bessaïs, M. Hajji, M. Kanzari, H. Ezzaouiaa, N. Hamdadoud, J.C. Bernède, Materials Letters 59 (2005) 734–739.
[12] R. Dasbach, G. Willeke, O. Blenk, MRS Bull. 18 (10) (1993) 56–60.
[13] A. Ennaoui, S. Fiechter, W. Jaegermann, H. Tributsch, J. Electrochem. Soc. 133 (1)(1986) 91–106.
[14] K. Buker, N. Alnonso-Vante, H. Tributsch, J. Appl. Phys. 72 (1992) 5721–5728.
[15] N. Alonso-Vante, G. Chatzitheodorou, S. Fiechter, N. Mgoduka, I. Poulios, H. Tributsch, Sol. Energy Mater. 18 (1988) 9–21.
[16] R. Sun, G. Ceder, Phys. Rev. B 84 (2011) 245211–245217.
[17] S.W. Lehner, K.S. Savage, J.C. Ayers, J. Cryst. Growth 286 (2006) 306–317.
[18] I.J. Ferrer, F. Cabalerro, C. De las Heras, C. Sanchez, Solid State Commun. 89 (1994) 349–352.

International Journal of Engineering Research & Technology (IJERT)
ISSN: 2278-0181
Vol. 9 Issue 05, May-2020

[19] Beya Ouertani, Hatem ezzaouia, and Bertran Tess , Colloids and Surfaces A 525 (2017) 13–19.
[20] P. Xiao, X.-L. Fan, H. Zhang, X. Fang, L.-M. Liu, J. Alloys Compd. 629 (2015) 43–48.
[21] Jibo Jiang,Liying Zhu,Haotian Chen,Yaoxin Sun,Hualin Lin, and ShengHan, Journal of Alloys and Compounds,Volume 775, 15 February 2019, Pages 1293-1300
[22] YangDing, PeiyuanZeng, and ZhenFang,Journal of Power Sources,Volume 450, 29 February 2020, 227688
[23] Xing-HuaTian, and Jian-MinZhang, Materials Chemistry and Physics, Volume 239, 1 January 2020, 122057
[24] N.Ouarab, Physica E: Low-dimensional Systems and Nanostructures,Volume 115, January 2020, 113688